

Instability analysis of spin-electron-acoustic waves and the appearance of separated spin electron cyclotron mode in spin-polarized magnetized quantum plasma

Nabi Gul¹ and Rashid Ahmad^{2,*}

¹Department of Physics, Govt. Degree College Darra Adam Khel, Kohat 26000, Khyber Pakhtunkhwa, Pakistan

²Department of Physics, Kohat University of Science and Technology, Kohat 26000, Khyber Pakhtunkhwa, Pakistan



(Received 18 March 2022; revised 2 July 2022; accepted 9 August 2022; published 30 August 2022)

Linear and nonlinear characteristics of electrostatic waves are studied in a magnetized plasma consisting of spin-up (n_{\uparrow}) and spin-down (n_{\downarrow}) state populations with uniformly distributed static ions in the background. The linear analysis shows the existence of four modes. One of these modes, termed the separated spin electron cyclotron wave, is found to be due to the separated spin populations. The Zakharov-Kuznetsov equation is derived by the reductive perturbation technique. The instability growth rate γ is obtained from the same equation. It is observed that the magnetized spin quantum plasma admits rarefactive soliton with constant amplitude but increasing width with the increasing strength of the applied magnetic field. It has also been observed that the amplitude of soliton decreases and its width increases with the increasing values of polarization ratio κ . The unstable region expands with the increase in polarization ratio and contracts with the increased plasma number density and magnetic-field strength. The (growth rate) γ of instability reduces by increasing the κ and is increasing when the density of the plasma and the strength of the magnetic field increasing. The model developed in this work finds its scope in studying degenerate electron gas and astrophysical systems such as pulsar magnetosphere and neutron stars.

DOI: [10.1103/PhysRevE.106.025206](https://doi.org/10.1103/PhysRevE.106.025206)

I. INTRODUCTION

Quantum effects in plasma is a topic of interest among the plasma physics community for over six decades now [1,2]. It is commonly described as a multicomponent system of charged particles in which at least one of the constituent components (in many cases the electrons) exhibits degeneracy. The degeneracy of particles means that the Pauli exclusion principle is important in such systems and that the spin and exchange effect must be considered. The spin effect is significant if the energy difference between the two spin states is greater than the thermal or Fermi energy [i.e., $(\frac{\mu_B B_0}{k_B T}) \leq 1$ or $(\frac{\mu_B B_0}{k_B T_F}) \leq 1$] [3–5] here, μ_B is the magnetic moment and T_F is the Fermi temperature of electron. Thus, for spin effects to be important, we need low temperatures or extremely high magnetic fields. For example, in laboratory plasma, where magnetic fields $B_0 \approx 10\text{--}20$ T, we need low-temperature plasmas for the spin effects to influence the properties of plasma. However, we have $B_0 \approx 10^8\text{--}10^{13}$ Gs in the vicinity of pulsars and magnetars [6]. Spin effects can be significant in such systems, even in a high-temperature (high density) plasma [7]. The external magnetic field influences the occupancy of quantum states by spin-up and spin-down electrons. In high-density plasma the spin-up and spin-down polarization degree is defined through relation $\kappa = (\frac{\mu_B B_0}{k_B T_F})$ [8]. The effect of Coulomb exchange interaction in quantum plasma was studied in Refs. [9,10]. In these references the constituent of plasma was considered as spin-less particles. The additional contribution due to the spin-spin interaction was later incorporated in Refs. [11–13] by

considering the plasma consisting of spin-1/2 particles. Marklund and Brodin demonstrated significant alteration in the low-frequency modes provided the matching conditions for spin-plasma were met [7,14]. The inclusion of the spin effect was also shown to have modified the dispersion of linear wave propagation in an electron-ion plasma [14]. When the spins in a strongly magnetized plasma are aligned with the magnetic field, a relatively small spin force becomes important, causing the weakly nonlinear shear Alfvén waves governed by the modified Korteweg–de Vries equation leading to soliton formation [15]. Obliquely propagating magnetosonic waves were investigated in the paper [16] by considering the spin effects and Bohm potential. Misra *et al.* have observed that the inclusion of spin influenced the dispersion while studying the propagation of circularly polarized electromagnetic waves through a magnetized spin plasma [17]. They also observed a new high-frequency eigenmode (circularly polarized) [17]. This influence was found to be very high when the magnetic field is large and density is the high relativistic case. Even in the nonrelativistic cases, when the magnetic field is not so high ($B_0 < B_Q \equiv 4.4138 \times 10^9$ T) but the plasma density is high ($n_0 \gg n_c \simeq 10^{32}$ m⁻³), the influence of spin inclusion was found to be substantial. In the presence of intrinsic magnetization, a novel type of instability was observed in plasmas [18] using the quantum hydrodynamic (QHD) model. It was shown that Alfvén waves make a crucial contribution in causing this instability when the number density of plasma and electron temperature varies along the external magnetic field [18].

Separated spin development of electrons in plasmas results in the appearance of new interesting wave modes, for example, the electron quantum states of different spin densities

*rashidahmad@kust.edu.pk

correspond to separated spin states equations, which further plays an essential role in plasma waves dispersion [19–23]. Furthermore, it was demonstrated that taking into account the different spin electron populations state resulted in the discovery of a novel longitudinal wave [20]. Detailed quantum hydrodynamics of separated spin population reveals the occurrence of electron acoustic waves with separated spin in Ref. [21]. Electrostatic as well as nonlinear solitary waves having both types of electrons states in quantum plasma were explored in Refs. [23–26]. The different electrons populations alter the Columbic exchange interaction. Recently, interest is growing in dynamics of spin particles and exchange interactions, see Refs. [13,27–32]. These works are concerned with the lengthy histories of the Coulomb exchange interaction [33–35], and applying exchange interaction to several plasma processes [36,37].

In this paper, the previous work of Andreev [21] is extended to explore properties of electrostatic solitary pulses in plasma containing degenerate spin population of electrons. For simplicity, taking into account the spin-exchange force in spin-down electrons only. The reductive perturbation technique (RPT) is implemented to derive a nonlinear Zakharov-Kuznetsov (ZK) type equation for solitary waves profiles. According to the work of Allen and Rowlands [38,39], it is demonstrated that the ZK equation admits the unstable pulse solitary solution under oblique perturbations. The growth rate instability depends on several parameters that are analytically explored.

The structure of this article goes as follows: In Sec. II of this paper, the hydrodynamic model of separated spin electrons in magnetized quantum plasma having electrostatic excitations are described. The nonlinear analysis of spin separated acoustic-wave is performed in Sec. III and derives a ZK-type equation. In its section, solitary waves solution is presented. The results are parametrically displayed and explained in terms of several plasma properties. The analysis of the stability of waves resulting from the ZK equation is investigated in Sec. V. The conclusion of the work is added in Sec. VI.

II. MATHEMATICAL MODEL

The development of the QHD model of quantum plasmas containing spinning particles has a long history. Various methods for generating QHD equations have been reported [40,41] and have also been utilized for quantum plasmas containing spinning particles [42,43]. An attempt was made to construct the quantum hydrodynamic model of particles with spin-up and spin-down concentrations [44], this approach has found a variety of applications [4,18,45–49]. In an other approach the quantum hydrodynamic for separated spins model is obtained directly from the *Pauli* equation [21]. The *Pauli* equation contains the development of two wave functions: one for an electron's spin-up state and another for its spin-down state, the spin-up and spin-down states being treated as two different species of an electron. Therefore this model is known as the separated-spin evolution quantum hydrodynamic model. This many-particle quantum hydrodynamics can be simplified by considering the *Pauli* equation for a single particle in an external electromagnetic field, which approximately cor-

responds with the single-particle QHD [50]. However, the many-particle formalism known as many-particle QHD has been heavily used over the last decade, e.g., in Refs. [7,51].

The *separated spin electron quantum-hydrodynamics model* (SSE-QHD) [21] is used to examine the dispersive and solitary wave properties of magnetized quantum plasma consisting electrons with spin-up (n_\uparrow) and spin-down (n_\downarrow); two separate populations state. An external magnetic field is applied along the z axis, i.e., $\mathbf{B} = B_0\hat{z}$. In the presence of an electromagnetic wave propagating along the z direction, the motion of charged particles generates an internal magnetic field in B_x , B_y , and B_z . The SSE-QHD model consists of the following number density conservation (continuity) equation:

$$\frac{\partial n_s}{\partial t} + \nabla \cdot (n_s \mathbf{v}_s) = \pm \frac{\gamma_e}{\hbar} (B_y S_x - B_x S_y), \quad (1)$$

where s represents the spin-up (\uparrow) and spin-down (\downarrow) electron concentrations and \pm on the right-hand side of Eq. (1) denotes the spin-up and the spin-down electrons, respectively. γ_e is the electron gyromagnetic ratio defined by $\gamma_e = -g \frac{e\hbar}{2mc}$ and $g \simeq 1.00116$ for electrons. e and m are the electron charge and mass, c is the speed of light in free space, \hbar is the Planck constant divided by 2π , and S_x , S_y are spin components. According to the continuity equation (1), the number of electrons in each state is not constant due to spin interaction with the internal magnetic field of charged particles. However, in this approach, the total number of electrons $n_e = n_\uparrow + n_\downarrow$ is preserved in both states. The momentum equation of spin-up and spin-down electrons is

$$\begin{aligned} m_s n_s \left(\frac{\partial}{\partial t} + \mathbf{v}_s \cdot \nabla \right) \mathbf{v}_s &= -en_s \left(\mathbf{E} + \frac{B_0}{c} \mathbf{v}_s \times \hat{r} \right) - \nabla P_s + F_{Exs} \pm \gamma_e n_s \nabla B_z \\ &+ \frac{\gamma_e}{2} (S_x \nabla B_x + S_y \nabla B_y) \pm \frac{m\gamma_e}{\hbar} (J_{mx} B_y - J_{my} B_x) \\ &\mp \frac{mv_s \gamma_e}{\hbar} (B_y S_x - B_x S_y). \end{aligned} \quad (2)$$

To close the above-mentioned set of equations, the following *Maxwell* equations are required:

$$\begin{aligned} \nabla \cdot \mathbf{E} &= 4\pi e(n_{0i} - n_\downarrow - n_\uparrow), \quad \nabla \cdot \mathbf{B} = 0, \\ \nabla \times \mathbf{E} &= -\frac{1}{c} \frac{\partial \mathbf{B}}{\partial t}, \\ \nabla \times \mathbf{B} &= \frac{1}{c} \frac{\partial \mathbf{E}}{\partial t} + 4\pi \nabla \times \mathbf{M} - \frac{4\pi e}{c} \sum_s (n_s \mathbf{v}_s), \end{aligned} \quad (3)$$

where n_s and v_s are the spin-up and spin-down state electron number densities and electron fluid velocities, respectively. The intensity of the electric field \mathbf{E} is $\mathbf{E} = -\nabla\phi$, where ϕ is the electrostatic scalar potential. The pressures terms for spin-up and spin-down degenerate electrons are, respectively [21], $P_s = \frac{K_B T_{Fs} n_s^{5/3}}{5n_{0s}^{2/3}}$, where $T_{Fs} = \frac{(6\pi^2 n_{0s})^{2/3} \hbar^2}{2K_B m}$ is the Fermi scale temperatures of electron and K_B is the *Boltzmann* constant. \mathbf{M} is spin magnetization term of the electron in terms of components [$\mathbf{M} = \gamma_e S_x, \gamma_e S_y, \gamma_e (n_\uparrow - n_\downarrow)$] For simplicity the term F_{Exs} in Eq. (2) represents the spin interaction force of the spin-down electrons only. This force are the resulting from

the exchange of spin density, in terms of spin polarization $\kappa = \frac{n_{0\uparrow} - n_{0\downarrow}}{n_{0\uparrow} + n_{0\downarrow}}$, $\kappa \in [0, 1]$ is given by

$$\mathbf{F}_{Ex,\downarrow} = \chi e^2 n_{\downarrow}^{1/3} \nabla n_{\downarrow}, \quad (4)$$

where

$$\chi = 2^{4/3} (3/\pi)^{1/3} \left(1 - \frac{(1-\kappa)^{4/3}}{(1+\kappa)^{4/3}} \right). \quad (5)$$

The spin current elements J_{mx} and J_{my} can define the following explicit forms:

$$J_{mx} = \frac{1}{2} (v_{\uparrow} + v_{\downarrow}) S_x - \frac{\hbar}{4m} \left(\frac{\nabla n_{\uparrow}}{n_{\uparrow}} - \frac{\nabla n_{\downarrow}}{n_{\downarrow}} \right) S_y, \quad (6)$$

$$J_{my} = \frac{1}{2} (v_{\uparrow} + v_{\downarrow}) S_y + \frac{\hbar}{4m} \left(\frac{\nabla n_{\uparrow}}{n_{\uparrow}} - \frac{\nabla n_{\downarrow}}{n_{\downarrow}} \right) S_x. \quad (7)$$

The spin current density J_{mx} , J_{my} and magnetization current density M_x , M_y are produced due to the internal magnetic field of moving charged particles. The presented model is a two-fluid model in which electrons are supposed to have two different orientations with spin-up and spin-down states with respect to uniform external magnetic field. When the plasmas are characterized by a single electron population with a background spin distribution approaching thermodynamic equilibrium, the spin effects are constrained to some extent whenever $\frac{\mu_B B_0}{k_B T} \leq 1$. Thus, low temperatures or extremely high magnetic fields are necessary for spin effects to be considerable in the single electron fluid model [52]. On the other hand, separated spin evolution of electrons may be important in a weakly magnetized high-temperature plasma inside the two-fluid electron model [4,18]. Two approaches were developed: kinetic and fluid (bulk) to describe the dynamic of spin quantum plasma. The kinetic model is considerably simplified at macroscopic scale lengths greater than the typical de Broglie wavelength. References [18,52–55] provide a concise summary of various different plasma models for dealing with spin magnetization effects, spin coupling, and spin-spin interaction in plasmas, with an emphasis on recent advancements, and the link behind the conceptual transition from kinetic to fluid models is discussed in detail.

In the absence of an internal magnetic field $B_x = 0$, $B_y = 0$, and $B_z = 0$ the simplified and normalized dynamical equations for the spin-up and spin-down state populations of electrons fluid when the external magnetic field is applied along the z axis, i.e., $\mathbf{B} = B_0 \hat{z}$, as in the following form:

$$\frac{\partial n_{\uparrow}}{\partial t} + \nabla \cdot (n_{\uparrow} \mathbf{v}_{\uparrow}) = 0, \quad (8)$$

$$\frac{d}{dt} \mathbf{v}_{\uparrow} = \nabla \phi - \Omega_c \mathbf{v}_{\uparrow} \times \hat{z} - \frac{(2\delta_{\uparrow})^{2/3}}{3} n_{\uparrow}^{-1/3} \nabla n_{\uparrow}, \quad (9)$$

$$\frac{\partial n_{\downarrow}}{\partial t} + \nabla \cdot (n_{\downarrow} \mathbf{v}_{\downarrow}) = 0, \quad (10)$$

$$\frac{d}{dt} \mathbf{v}_{\downarrow} = \nabla \phi - \Omega_c \mathbf{v}_{\downarrow} \times \hat{z} - \frac{(2\delta_{\downarrow})^{2/3}}{3} n_{\downarrow}^{-1/3} \nabla n_{\downarrow} + \Gamma n_{\downarrow}^{-2/3} \nabla n_{\downarrow}, \quad (11)$$

$$\nabla^2 \phi = \delta_{\uparrow} n_{\uparrow} + \delta_{\downarrow} n_{\downarrow} - 1, \quad (12)$$

where d/dt includes time and convective derivatives defined as $d/dt = (\partial/\partial t + \mathbf{v}_{\uparrow,\downarrow} \cdot \nabla)$.

Here, $\delta_{\uparrow} = n_{0\uparrow}/n_0$, $\delta_{\downarrow} = n_{0\downarrow}/n_0$ are equilibrium density ratio. $\Omega_c (= \omega_{ce}/\omega_{pe})$ is the normalized cyclotron frequency of electron, where $\omega_{ce} (= \frac{eB_0}{m_e c})$ and $\omega_{pe} [= (4\pi n_0 e^2 / m_e)^{1/2}]$ are the cyclotron and plasma frequencies of electrons, respectively. The number densities n_{\uparrow} and n_{\downarrow} are scaled by their corresponding equilibrium number densities, the velocities of fluid \mathbf{v}_{\uparrow} and \mathbf{v}_{\downarrow} are normalized by the electron-acoustic speed $c_s (= \sqrt{2k_B T_F / m_e})$, and the scalar electrostatic potential ϕ is normalized with $2k_B T_F / e$. The space coordinates are normalized with the electronic skin length $\lambda_e (= \frac{c_s}{\omega_{pe}})$ and time is scaled with the inverse of the electron plasma frequency ω_{pe} . Here $T_F = (3\pi^2 n_0)^{2/3} \hbar^2 / (2k_B m_e)$ is the electron Fermi temperature. We can write the spin density ratio δ_s in terms of density polarization κ as $\delta_{\uparrow} = n_{0\uparrow}/n_{i0} = (1+\kappa)/2$ and $\delta_{\downarrow} = n_{0\downarrow}/n_{i0} = (1-\kappa)/2$, the index s signifies the spin-up and spin-down states of electrons. The last term in Eq. (11) contains the normalized spin-density interaction of spin-down electrons and is given by

$$\Gamma = \frac{\chi e^2 m_e}{\hbar^2 (2\pi^2)^{3/2} n_0^{1/3}} \left(\frac{1+\kappa}{2} \right)^{1/3}. \quad (13)$$

The authors would like to refer to Fig. 1 of Refs. [23,31], which provides a detailed description of the spin-density interaction and its importance in the spin state.

A. Linear analysis and dispersion relation

By using Fourier analysis, we linearize the system of Eqs. [(8)–(12)] by assuming variation of the dynamical variables of the form $\sim e^{i(\mathbf{k}\cdot\mathbf{r} - \omega t)}$. Replace $\partial/\partial x$ with ik_x , $\partial/\partial y$ with ik_y , $\partial/\partial z$ with ik_z , and $\partial/\partial t$ with $-i\omega$ in Eqs. (8)–(12), and then with some algebraic manipulation, we get the following dispersion relations for longitudinal and transverse directions, respectively:

$$1 = \frac{(1+\kappa)}{2(\omega^2 - \frac{k^2(1+\kappa)^{2/3}}{3})} + \frac{(1-\kappa)}{2(\omega^2 - \frac{k^2(1-\kappa)^{2/3}}{3} + k^2\Gamma)}, \quad (14)$$

$$1 = \frac{(1-\kappa)}{2(\omega^2 - \Omega^2 - \frac{k^2(1-\kappa)^{2/3}}{3} + k^2\Gamma)} + \frac{(1+\kappa)}{2(\omega^2 - \Omega^2 - \frac{k^2(1+\kappa)^{2/3}}{3})}. \quad (15)$$

Equation (14) indicates the dispersive properties of the separated spin evolution plasma in the longitudinal direction. Due to the separate spin evolution of the spin-up and spin-down state, a new wave mode appears called separated spin electron acoustic waves and has been treated in detail in Ref. [21]. Equation (15) shows the dispersive properties of the separated spin evolution plasma in the transverse direction. The solution of Eq. (15) contains two roots relating to the upper hybrid and the separated spin electron cyclotron modes. The appearance of novel electron cyclotron waves is attributed to the separate spin consideration of electrons populations.

Figure 1 shows the relationship between the normalized wave frequency ω (scaled by ω_{pe}) and the magnitude of normalized propagation wave vector k (scaled by λ_e) for various plasma parameters. The plots in Fig. 1(a) are for fixed values of the normalized cyclotron frequency of electron, $\Omega = 0.6$, spin-density polarization ratio $\kappa = 0.1$, and density

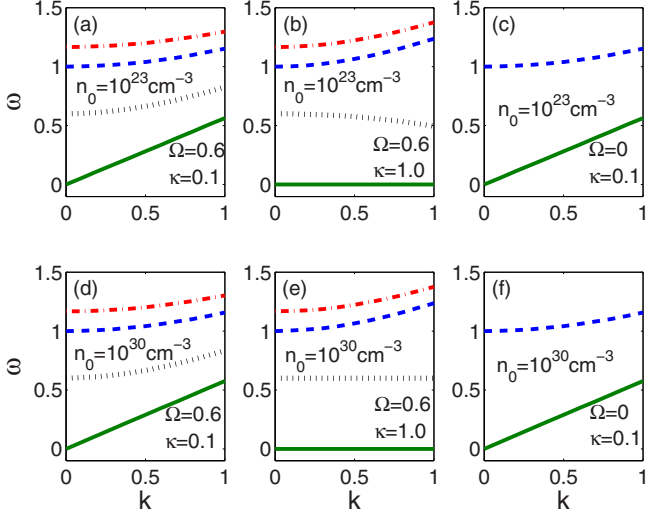


FIG. 1. The dispersion curves of all four modes are depicted by displaying the angular frequency ω (scaled by ω_{pe}) versus the wave vector k (scaled by λ_e), for the density of 10^{23} cm^{-3} (upper panel) and 10^{30} cm^{-3} the (lower panel). The normalized electron cyclotron frequency Ω is varied between 0 and 0.6 while the spin-density polarization κ is varied between 0.1 and 1.0. The solid curve represents the SSEAWs, the dashed curve represents the LWs, the dotted curve represents the SSECWs, and the dash-dotted curve represents the UHWs.

$n_0 = 10^{23} \text{ cm}^{-3}$; Fig. 1(b) $\Omega = 0.6$, $\kappa = 1$, i.e., only one kind of electron (either spin-up or spin-down), and $n_0 = 10^{23} \text{ cm}^{-3}$; Fig. 1(c) $\Omega = 0$, i.e., unmagnetized plasma, $\kappa = 0.1$, and $n_0 = 10^{23} \text{ cm}^{-3}$; Fig. 1(d) $\Omega = 0.6$, $\kappa = 0.1$, and $n_0 = 10^{30} \text{ cm}^{-3}$; Fig. 1(e) $\Omega = 0.6$, $\kappa = 1$, and $n_0 = 10^{30} \text{ cm}^{-3}$; and Fig. 1(f) $\Omega = 0$, $\kappa = 0.1$, and $n_0 = 10^{30} \text{ cm}^{-3}$. According to Figs. 1(a) and 1(d), our spin polarized magnetized quantum plasma exists four modes of waves. The Langmuir waves (LWs) is the dashed curve that starts at the electron plasma frequency (ω_{pe}) is the Langmuir wave (LW). The dash-dotted curve which is at the highest frequency mode represent the upper hybrid waves (UHWs). The dotted curve belongs to the separated spin electron cyclotron waves (SSECWs). The separated spin electron-acoustic wave is shown by the solid curve that begins at the lowest frequency (SSEAW). Figures 1(b) and 1(e) indicate the plasma case with the switch off-spin density polarization i.e. and contain only one species of electrons (either spin-up or spin-down). We can observe that in this case, the two modes associated with the evolution of separated spin electrons, i.e., SSECWs and SSEAWs, become oscillatory only, which make the confirmation of existence and propagation of these modes only due to spin polarization. When we turn off the external magnetic field ($\Omega = 0$), the two modes UHWs and SSECWs vanish, as seen in Figs. 1(c) and 1(f).

Figure 2 shows the plots between ω and k for different values of spin-density polarization ratio $\kappa = 0.1, 0.3, 0.6$ and at a fixed value of $\Omega = 0.6$. The subplots in the top row show the dispersion of SSEAW by taking n_0 as $10^{23}, 10^{26}, 10^{30} \text{ cm}^{-3}$ in Figs. 2(a)–2(c), respectively, whereas the subplots of the bottom row show the dispersion of SSECW for

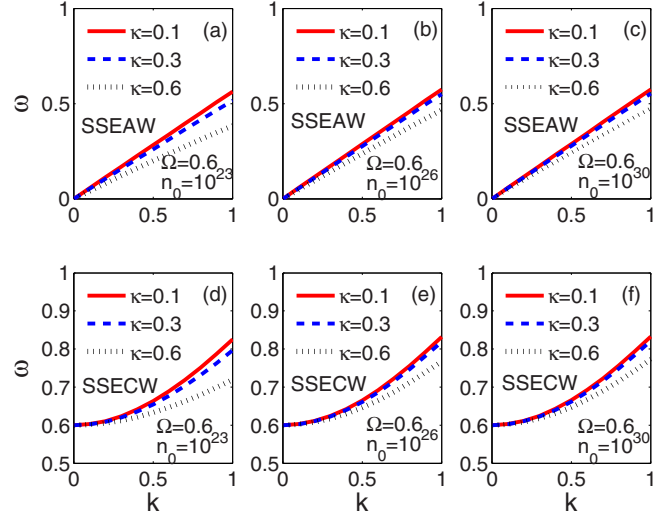


FIG. 2. Dispersion curves depicting the angular frequency ω (scaled by ω_{pe}) versus the wave vector k (scaled by λ), the upper panel is for the SSEAW while the lower panel is for the SSECW, both for a fixed value of $\Omega = 0.6$. The solid curve is for $\kappa = 0.1$, the dashed curve is for $\kappa = 0.3$, and the dotted curve is for $\kappa = 0.6$.

n_0 as $10^{23}, 10^{26}, 10^{30} \text{ cm}^{-3}$ in Figs. 2(d)–2(f), respectively. We see from Fig. 2(a) that the phase velocity of SSEAW decreases with the increasing values of κ for fixed value of electron number density. This decrease in the phase velocity is larger for the highest value of κ . When we increase the value of n_0 , the difference in the phase velocity decreases as shown in Fig. 2(b). The subplots in the lower panel Figs. 2(d) and 2(f) show that the phase velocity of SSECW shows similar decreasing dependence with the increasing values of κ for different values of n_0 .

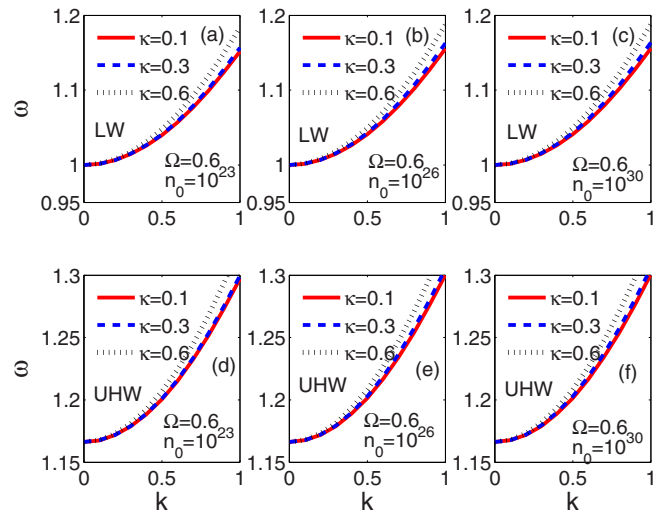


FIG. 3. Dispersion curves depicting the angular frequency ω (scaled by ω_{pe}) versus the wave vector k (scaled by λ), the upper panel is for the LW while the lower panel is for the UHW, both for a fixed value of $\Omega = 0.6$. The solid curve is for $\kappa = 0.1$, the dashed curve is for $\kappa = 0.3$, and the dotted curve is for $\kappa = 0.6$.

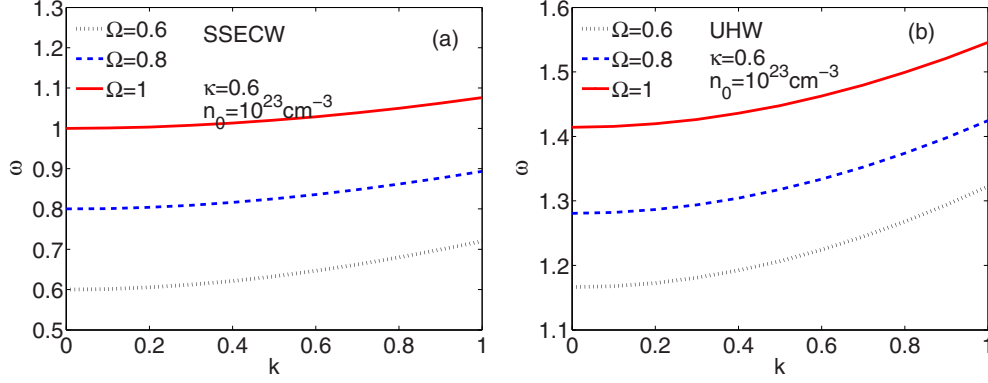


FIG. 4. Dispersion curves depicting the angular frequency ω (scaled by ω_{pe}) versus the wave vector k (scaled by λ), for (a) the SSECW and (b) the UHW, at fixed values of $\kappa = 0.6$ and density $n_0 = 10^{23} \text{ cm}^{-3}$. The solid curve is for $\Omega = 1.0$, the dashed curve is for $\Omega = 0.8$, and the dotted curve is for $\Omega = 0.6$.

Figure 3 shows the plots between ω and k for different values of density polarization ratio $\kappa = 0.1, 0.3, 0.6$ and at $\Omega = 0.6$. The subplots in the top row show the dispersion of LW by taking n_0 as $10^{23}, 10^{26}, 10^{30} \text{ cm}^{-3}$ in Figs. 3(a)–3(c), respectively, whereas the subplots of the bottom row show the dispersion of UHW for n_0 as $10^{23}, 10^{26},$ and 10^{30} cm^{-3} in Figs. 3(d)–3(f), respectively. We see from Fig. 3(a) that the phase velocity of LW increases with the higher values of κ at a given value of n_0 . The dispersion curves for LW do not change with higher values of electron number density, as can be seen in Figs. 3(b) and 3(c). The phase velocity of UHW shows similar increasing behavior with the higher values of κ but remains constant with increasing values of n_0 , as can be seen in Figs. 3(d)–3(f), respectively. We also observed that the phase velocity of the UHW is a little larger compared with the phase velocity of LW. Figure 4 shows the effect of external magnetic field through Ω on the dispersion curves of SSECW and UHW. In both figures we have used $\kappa = 0.6$ and $n_0 = 10^{23} \text{ cm}^{-3}$. Figures 4(a) and 4(b) show that the normalized frequency ω of SSECW and UHW increases with the higher values of the external magnetic field.

III. NONLINEAR ANALYSIS

We use the standard reductive perturbation technique (RPT) [56] to explore the nonlinear propagation of separated spin electron acoustic waves in magnetized quantum plasma with static ions in the background. We consider the plasma to be three dimensional and suppose that the excitation evolves and propagates in the xz plane, thus, $\nabla = (\partial_x, 0, \partial_z)$. The space and time variables are stretched as $X = \epsilon^{1/2}x$, $Y = \epsilon^{1/2}y$, $Z = \epsilon^{1/2}(z - v_p t)$, and $T = \epsilon^{3/2}t$, where ϵ is a small parameter measuring the nonlinearity and v_p is the normalized phase velocity. The dynamical variables are defined as follows:

$$\begin{aligned} \phi &= \epsilon\phi^{(1)} + \epsilon^2\phi^{(2)} + \dots, & v_z &= \epsilon v_z^{(1)} + \epsilon^2 v_z^{(2)} + \dots, \\ v_{x,y} &= \epsilon^{3/2} v_{x,y}^{(1)} + \epsilon^2 v_{x,y}^{(2)} + \dots, \\ n &= 1 + \epsilon n^{(1)} + \epsilon^2 n^{(2)} + \dots. \end{aligned} \quad (16)$$

By using the stretching frame coordinates system along with the expansions of Eq. (16) in the scalar equations, Eqs. (8)–

(12), and equating the terms in different powers of ϵ , we get different equations. The following equations are obtained to the lowest order in ϵ :

$$\begin{aligned} \frac{\partial n_{\uparrow}^{(1)}}{\partial Z} &= \frac{3}{((1+\kappa)^{2/3} - 3v_p^2)} \frac{\partial \phi^{(1)}}{\partial Z}, \\ \frac{\partial v_{\uparrow z}^{(1)}}{\partial Z} &= \frac{3v_p}{((1+\kappa)^{2/3} - 3v_p^2)} \frac{\partial \phi^{(1)}}{\partial Z}, \end{aligned} \quad (17)$$

$$\begin{aligned} \frac{\partial n_{\downarrow}^{(1)}}{\partial Z} &= \frac{3}{((1-\kappa)^{2/3} - 3\Gamma - 3v_p^2)} \frac{\partial \phi^{(1)}}{\partial Z}, \\ \frac{\partial v_{\downarrow z}^{(1)}}{\partial Z} &= \frac{3v_p}{((1-\kappa)^{2/3} - 3\Gamma - 3v_p^2)} \frac{\partial \phi^{(1)}}{\partial Z}, \end{aligned} \quad (18)$$

$$\begin{aligned} v_{\uparrow x}^{(1)} &= \frac{3v_p^2}{\Omega((1+\kappa)^{2/3} - 3v_p^2)} \frac{\partial \phi^{(1)}}{\partial Y}, \\ v_{\uparrow y}^{(1)} &= -\frac{3v_p^2}{\Omega((1+\kappa)^{2/3} - 3v_p^2)} \frac{\partial \phi^{(1)}}{\partial X}, \end{aligned} \quad (19)$$

$$\begin{aligned} v_{\downarrow x}^{(1)} &= \frac{3v_p^2}{\Omega((1-\kappa)^{2/3} - 3\Gamma - 3v_p^2)} \frac{\partial \phi^{(1)}}{\partial Y}, \\ v_{\downarrow y}^{(1)} &= -\frac{3v_p^2}{\Omega((1-\kappa)^{2/3} - 3\Gamma - 3v_p^2)} \frac{\partial \phi^{(1)}}{\partial X}, \end{aligned} \quad (20)$$

$$\delta_{\uparrow} n_{\uparrow}^{(1)} + \delta_{\downarrow} n_{\downarrow}^{(1)} = 0. \quad (21)$$

From Eqs. (17), (18), and (21), we get the following expression for the phase velocity v_p :

$$v_p = \sqrt{\frac{(1-\kappa)(1+\kappa)^{2/3} + (1+\kappa)((1-\kappa)^{2/3} - 3\Gamma)}{6}}. \quad (22)$$

Equation (22) demonstrates that the phase velocity is dependent on the spin-density polarization κ and the spin interaction force. Using first-order perturbed quantity and the next order of ϵ , and using the first-order perturbed quantity, we derive a nonlinear partial differential equation in the form of the ZK

equation:

$$\frac{\partial \phi}{\partial T} + A\phi \frac{\partial \phi}{\partial Z} + B \frac{\partial^3 \phi}{\partial Z^3} + C \frac{\partial}{\partial Z} \left(\frac{\partial^2 \phi}{\partial X^2} + \frac{\partial^2 \phi}{\partial Y^2} \right) = 0. \quad (23)$$

Here, we have used $\phi = \phi^{(1)}$ for convenience. The real coefficients $A = b/a$ which accounting for nonlinearity, $B = 1/(2a)$, and $C = c/(2a)$ for dispersion are given by

$$a = \left(\frac{9v_p(1+\kappa)}{2((1+\kappa)^{2/3} - 3v_p^2)^2} + \frac{9v_p(1-\kappa)}{2((1-\kappa)^{2/3} - 3\Gamma - 3v_p^2)^2} \right), \quad (24)$$

$$b = \frac{1}{4} \left(\frac{81v_p^2(1+\kappa)}{((1+\kappa)^{2/3} - 3v_p^2)^3} + \frac{81v_p^2(1-\kappa)}{((1-\kappa)^{2/3} - 3\Gamma - 3v_p^2)^3} - \frac{3(1+\kappa)^{5/3}}{((1+\kappa)^{2/3} - 3v_p^2)^3} - \frac{3(1-\kappa)^{5/3}}{((1-\kappa)^{2/3} - 3\Gamma - 3v_p^2)^3} + \frac{36(1-\kappa)\Gamma}{((1-\kappa)^{2/3} - 3\Gamma - 3v_p^2)^3} \right), \quad (25)$$

and

$$c = \left(1 + \frac{9v_p^2(1+\kappa)}{2\Omega^2((1+\kappa)^{2/3} - 3v_p^2)^2} + \frac{9v_p^2(1-\kappa)}{2\Omega^2((1-\kappa)^{2/3} - 3\Gamma - 3v_p^2)^2} \right). \quad (26)$$

IV. SOLITARY WAVE SOLUTIONS OF ZAKHAROV-KUZNETSOV EQUATION

To investigate the characteristics of the separated spin electron acoustic solitary waves propagation along a direction that makes an angle θ with the Z axis, i.e., with the ambient magnetic field, and lies in the XZ plane, the coordinate axes X and Z are rotated through an angle θ , with the Y axis kept fixed. Thus, our independent variables transform according to [57–59] as

$$\begin{aligned} \xi &= X \sin \theta + Z \cos \theta, & \tau &= T, \\ \zeta &= X \cos \theta - Z \sin \theta, & \eta &= Y. \end{aligned}$$

Using the preceding transformations, the transformed ZK equation of Eq. (23) is obtained in the following form:

$$\begin{aligned} \frac{\partial \Phi}{\partial \tau} + \delta_1 \Phi \frac{\partial \Phi}{\partial \xi} + \delta_3 \Phi \frac{\partial \Phi}{\partial \zeta} + \delta_2 \frac{\partial^3 \Phi}{\partial \xi^3} + \delta_4 \frac{\partial^3 \Phi}{\partial \zeta^3} + \delta_5 \frac{\partial^3 \Phi}{\partial \xi^2 \partial \zeta} \\ + \delta_6 \frac{\partial^3 \Phi}{\partial \zeta^2 \partial \xi} + \delta_7 \frac{\partial^3 \Phi}{\partial \xi \partial \eta^2} + \delta_8 \frac{\partial^3 \Phi}{\partial \zeta \partial \eta^2} = 0, \end{aligned} \quad (27)$$

where

$$\begin{aligned} \delta_1 &= A \cos \theta, & \delta_2 &= (B \cos^3 \theta + C \cos \theta \sin^2 \theta), \\ \delta_3 &= -A \sin \theta, & \delta_4 &= (-B \sin^3 \theta - C \cos^2 \theta \sin \theta), \\ \delta_5 &= a^{-1} \sin \theta \left(-\frac{3}{2} \cos^2 \theta - \frac{1}{2} c \sin^2 \theta + c \cos^2 \theta \right), \\ \delta_6 &= a^{-1} \cos \theta \left(\frac{3}{2} \sin^2 \theta + \frac{1}{2} c \cos^2 \theta - c \sin^2 \theta \right), \end{aligned}$$

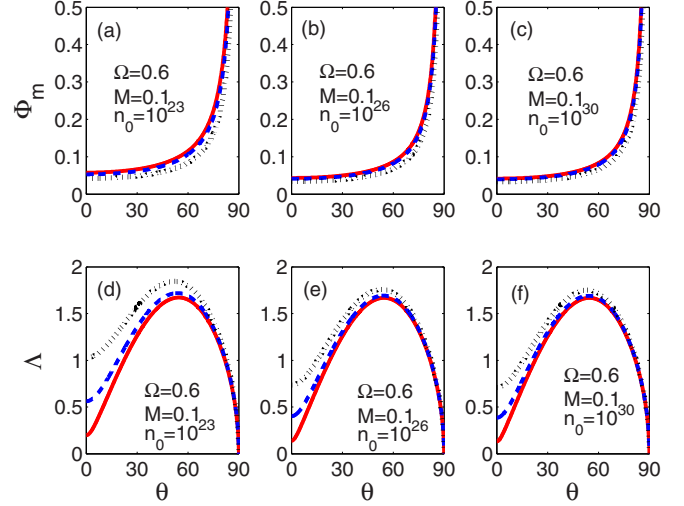


FIG. 5. Profiles of solitary waves displaying the amplitude Φ_m and width Λ of the soliton against the obliqueness angle θ for three different spin-density polarization ratios $\kappa = 0.1$ (solid line), $\kappa = 0.3$ (dashed line), and $\kappa = 0.6$ (dotted line), and for fixed values of $\Omega = 0.6$ and Mach No. $M = 0.1$.

$$\delta_7 = C \cos \theta, \quad \delta_8 = -C \sin \theta. \quad (28)$$

To obtain the stationary solution of the ZK equation (27), we change the independent variables ξ and τ to a single frame variable $\chi = \xi - M\tau$, where M is the Mach number, i.e., normalized frame velocity. Then Eq. (27) becomes

$$-M \frac{d\Phi}{d\chi} + \delta_1 \Phi \frac{d\Phi}{d\chi} + \delta_2 \frac{d^3 \Phi}{d\chi^3} = 0. \quad (29)$$

Now, using the boundary conditions, at $\chi \rightarrow \pm\infty$, then $\Phi \rightarrow 0$, $d\Phi/d\chi \rightarrow 0$, $d^2\Phi/d\chi^2 \rightarrow 0$, the Eq. (29) solitary wave solution is provided by

$$\phi = \phi_m \sec^2 \left(\frac{\chi}{\Lambda} \right), \quad (30)$$

where $\phi_m (=3M/\delta_1)$ is the amplitude and $\Lambda (=2\sqrt{\delta_2/M})$ is the width of the soliton.

The graph in Fig. 5 shows the amplitude Φ_m and width Λ of soliton versus the obliqueness angle θ for three different values of spin-density polarization ratios $\kappa = 0.1$ (solid line), $\kappa = 0.3$ (dashed line), and $\kappa = 0.6$ (dotted line). The upper panel row of subplots illustrates the variation of the amplitude of soliton Φ_m with changing values of plasma number density n_0 , using $\Omega = 0.6$ and $M = 0.1$. According to Fig. 5(a), the amplitude (Φ_m) grows slowly at first with rising values of the obliqueness angle θ up to $\theta = 60^\circ$ and then exponentially, reaching its maximum at around $\theta = 75^\circ$. As we increase κ values the amplitude decreases initially at smaller values of θ , but the curves overlap at about $\theta = 75^\circ$. From Figs. 5(b) and 5(c), we see similar behavior of Φ_m with θ for higher number densities as well. The lower panel of Fig. 5 depicts the width of soliton Λ for three different n_0 values. Figure 5(d), shows that, for a fixed constant value of κ , the width of soliton Λ grows with the obliqueness angle θ , reaching a maximum at around $\theta = 60^\circ$ and then decreasing to a minimum at $\theta = 90^\circ$. By raising the values of κ , we can observe that the width

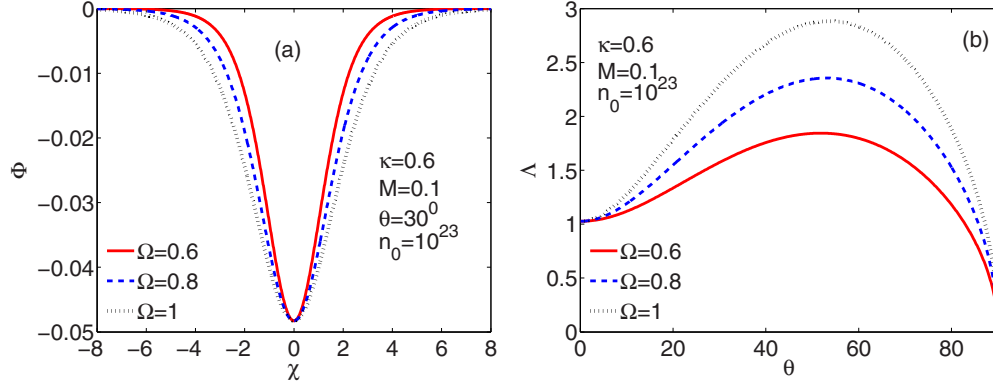


FIG. 6. Plots demonstrating the influence of varying magnetic field via Ω on (a) the soliton profile Φ vs χ curve, (b) the width of soliton Λ vs obliqueness angle θ , with constant values $\kappa = 0.6$, $M = 0.1$, $\theta = 30^\circ$, and $n_0 = 10^{23}$ cm $^{-3}$.

gradually increases and reaches a maximum at $\theta = 60^\circ$ and that beyond $\theta = 60^\circ$ different curves overlap and decrease at higher values of θ and almost vanish about $\theta = 90^\circ$. The width of soliton nearly exhibits the same behavior at greater number densities, as seen in Figs. 5(e) and 5(f), respectively. Figure 6 displays the impact of varying the magnetic-field strength through Ω on the soliton profile Φ [Fig. 6(a)] and the width of soliton Λ [Fig. 6(b)]. We see from Fig. 6(a) that the amplitude does not depend on the magnetic field. It is also obvious that our spin-polarized plasma permits only rarefactive soliton. From Fig. 6(b), we observed that the width of soliton Λ increases with increasing the strength of the magnetic field.

V. INSTABILITY ANALYSIS

In this section, we examine the instability of obliquely propagating separated spin electron acoustic solitary waves using the small- k perturbation expansion of Refs. [48,60,61]. We begin by assuming that

$$\phi^{(1)} = \phi_0(Z) + \phi(Z, \zeta, \eta, \tau). \quad (31)$$

For long-wavelength small- k sinusoidal waves perturbations having direction cosines (l, m, n) , then the $\phi(Z, \zeta, \eta, \tau)$ can be written as follows:

$$\phi(Z, \zeta, \eta, \tau) = \varphi(Z)e^{[ik(l\zeta + m\eta + nZ) - i\omega\tau]}, \quad (32)$$

where $l^2 + m^2 + n^2 = 1$. The $\varphi(Z)$ and ω may be extended for small k as

$$\begin{aligned} \varphi(Z) &= \varphi_0(Z) + k\varphi_1(Z) + k^2\varphi_2(Z) + \dots, \\ \omega &= k\omega_1 + k^2\omega_2 + \dots. \end{aligned} \quad (33)$$

Now, by plugging Eq. (31) into Eq. (27) and linearizing with regard to ϕ , then the linearized ZK equation may be written as follows:

$$\begin{aligned} \frac{\partial \phi}{\partial \tau} - M \frac{\partial \phi}{\partial Z} + \delta_1 \phi_0 \frac{\partial \phi}{\partial Z} + \delta_1 \phi \frac{\partial \phi_0}{\partial Z} + \delta_3 \phi_0 \frac{\partial \phi}{\partial \zeta} + \delta_2 \frac{\partial^3 \phi}{\partial Z^3} \\ + \delta_4 \frac{\partial^3 \phi}{\partial \zeta^3} + \delta_5 \frac{\partial^3 \phi}{\partial Z^2 \partial \zeta} + \delta_6 \frac{\partial^3 \phi}{\partial \zeta^2 \partial Z} + \delta_7 \frac{\partial^3 \phi}{\partial Z \partial \eta^2} \\ + \delta_8 \frac{\partial^3 \phi}{\partial \zeta \partial \eta^2} = 0. \end{aligned} \quad (34)$$

Equation (34) may be expressed as follows after using equation (32):

$$\begin{aligned} \left(-i\omega - iMkn + i\delta_1 k \phi_0 n + \delta_1 \frac{\partial \phi_0}{\partial Z} - ik\delta_2 k^3 n^3 + i\delta_3 k \phi_0 l \right. \\ \left. - i\delta_4 k^3 l^3 - i\delta_6 k^3 n l^2 - i\delta_7 k^3 n m^2 - i\delta_8 k^3 l m^2 \right) \varphi(Z) \\ + (-M + \delta_1 \phi_0 - 3\delta_2 k^2 n^2 - 2\delta_5 k^2 n l - \delta_6 k^2 l^2 - \delta_7 k^2 m^2) \\ \times \frac{\partial \varphi(Z)}{\partial Z} + (i3\delta_2 k n + i\delta_5 k l) \frac{\partial^2 \varphi(Z)}{\partial Z^2} + \delta_2 \frac{\partial^3 \varphi(Z)}{\partial Z^3} = 0. \end{aligned} \quad (35)$$

The following dispersion relation is derived by equating the coefficients of k up to second order:

$$\omega_1 = \Omega_1 - nM + \sqrt{(\Omega_1^2 - \Upsilon)}, \quad (36)$$

where

$$\Omega_1 = \frac{2}{3}(\phi_m \mu_1 - 2\mu_2^2 \Lambda^2), \quad (37)$$

and

$$\Upsilon = \frac{16}{45}(\phi_m^2 \mu_1^2 - 3\phi_m \mu_1 \mu_2 \Lambda^2 - 3\mu_2^2 \Lambda^4 + 12\delta_2 \mu_3 \Lambda^4). \quad (38)$$

μ_1 , μ_2 , and μ_3 are defined as

$$\mu_1 = (\delta_1 n + \delta_3 l), \quad \mu_2 = (3\delta_2 n + \delta_5 l), \quad (39)$$

$$\mu_3 = (3\delta_2 n^2 + 2\delta_5 l n + \delta_6 l^2 + \delta_7 m^2). \quad (40)$$

According to Eq. (36), plasma will be unstable if the following conditions are met:

$$(\Upsilon - \Omega_1^2) > 0. \quad (41)$$

Inserting Eqs. (37) and (38) into Eq. (41), we get

$$\begin{aligned} \frac{16}{45}(\Phi_m^2 \mu_1^2 - 3\Phi_m \mu_1 \mu_2 \Lambda^2 - 3\mu_2^2 \Lambda^4 + 12\delta_2 \mu_3 \Lambda^4) \\ - \left(\frac{2}{3}(\Phi_m \mu_1 - 2\mu_2^2 \Lambda^2) \right)^2 > 0. \end{aligned} \quad (42)$$

Using Eqs. (28) and (40), as well as Φ_m and Λ values in Eq. (42), we derive the instability criterion in its simplified form, which is written as

$$S = m^2(\cos^2 \theta + C \sin^2 \theta) + l^2(1 - \frac{5}{3}C \tan^2 \theta) > 0. \quad (43)$$

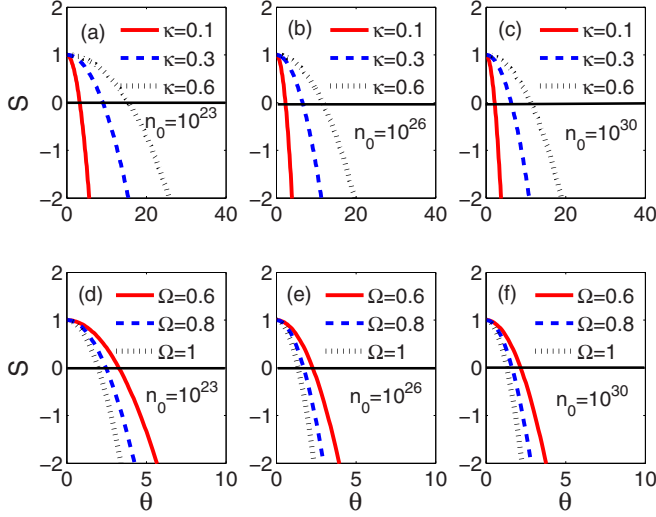


FIG. 7. The plot of Eq. (43) displaying S (instability region) vs the obliqueness angle θ demonstrating the impact of spin-density polarization ratio κ (upper panel), and the strength of external magnetic field through Ω (lower panel) for three distinct plasma number densities.

Equation (43) gives us the information about the instability region. We have a stable region when $S < 0$, while $S > 0$ gives us an unstable region.

Figure 7 depicts the relationship between S (the instability region) versus the propagation direction θ for various spin-density polarization ratios $\kappa = 0.1, 0.3, 0.6$ and $10^{23}, 10^{26}, 10^{30} \text{ cm}^{-3}$ [see Figs. 7(a)–7(c), respectively] and for different values of the strength of applied magnetic field $\Omega = 0.6, 0.8, 1$ and $10^{23}, 10^{26}, 10^{30} \text{ cm}^{-3}$ [see Figs. 7(d)–7(f), respectively]. We see from Fig. 7(a) that increasing the value of polarization ratio causes an increase in the range of the obliqueness angle θ for which the plasma remains unstable at a given value of plasma number density. An increase in the value of n_0 to 10^{26} cm^{-3} as in Fig. 7(b) results in the reduction of the range of θ for which the plasma

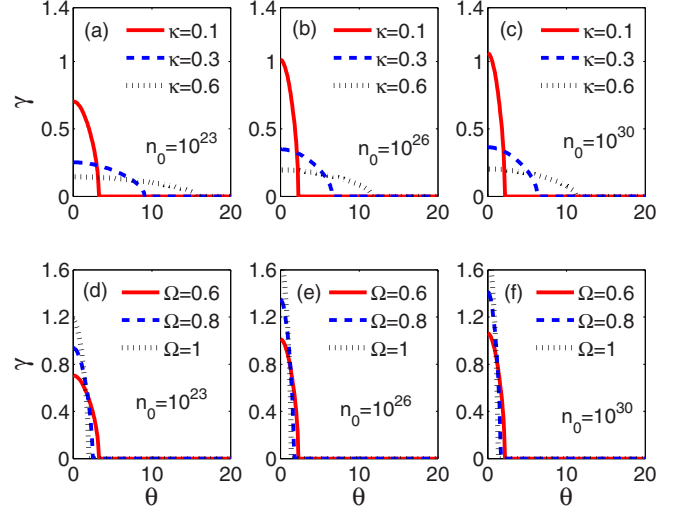


FIG. 8. Plots depicting the instability growth rate γ versus the obliqueness angle θ showing the effect of variation of spin-density ratio κ (upper panel), and the strength of external magnetic field via Ω (lower panel) for three different plasma number densities.

remains unstable. A further increase in the number density has a very small effect on the range of θ , as can be seen from Fig. 7(c). We see from Fig. 7(d) that increasing the magnitude of the magnetic field (higher values of Ω) decreases the range of θ for which the plasma is unstable at a fixed value of n_0 . It is clear from Fig. 7(e) that increasing the value of n_0 to 10^{26} cm^{-3} reduces the range of θ for which the plasma remains unstable. Further increase in the density does not affect the plasma unstable region, as can be seen from Fig. 7(f).

If Eq. (43) is satisfied, i.e., $S > 0$, then the growth rate γ of the unstable perturbation of the solitary-wave solution is given by

$$\gamma = \sqrt{\Upsilon - \Omega_1^2}. \quad (44)$$

Putting the values of Υ and Ω_1 in equation (44), we get

$$\gamma = \sqrt{\frac{16}{45}(\Phi_m^2 \mu_1^2 - 3\Phi_m \mu_1 \mu_2 \Lambda^2 - 3\mu_2^2 \Lambda^4 + 12\delta_2 \mu_3 \Lambda^4) - \left(\frac{2}{3}(\Phi_m \mu_1 - 2\mu_2^2 \Lambda^2)\right)^2}. \quad (45)$$

A simplified form of the growth rate of the above equation is

$$\gamma = \frac{2M}{\sqrt{15}} \sqrt{C \frac{[m^2(\cos^2 \theta + C \sin^2 \theta) + l^2(1 - \frac{5}{3}C \tan^2 \theta)]}{\cos^2 \theta + C \sin^2 \theta}}. \quad (46)$$

Figure 8 displays the relation between the growth rate γ and the obliqueness angle θ for three different values of spin polarization $\kappa = 0.1, 0.3, 0.6$ and for $10^{23}, 10^{26}, 10^{30} \text{ cm}^{-3}$ [see Figs. 8(a)–8(c), respectively], and for different values of the magnitude of the applied magnetic field $\Omega = 0.6, 0.8, 1$ and for $10^{23}, 10^{26}, 10^{30} \text{ cm}^{-3}$ [see Figs. 8(d)–8(f), respectively]. Figure 8(a) shows that there is an inverse relation between the growth rate γ and the propagation direction θ for a given values of the spin polarization κ . As we increase

the value of the spin polarization, the growth rate decreases but extends over a larger range of θ at a fixed value of n_0 . While increasing n_0 to 10^{26} cm^{-3} , the growth rate at different values of κ increases but the range of θ for which the instability occurs decreases, as can be seen in Fig. 8(b). Further increases in the value of n_0 cause a very minute increases in the growth rate, as can be seen in Fig. 8(c). The bottom row of Fig. 8 shows that the growth rate increases with the increasing strength of the applied magnetic field and plasma number density, whereas the range of θ decreases very slightly.

VI. CONCLUSIONS

From the application point of view, our findings are relatively general, with particular importance for the partially

spin-polarized plasmas such as dilute magnetic semiconductors, magnetosphere, and as well as astrophysical plasmas. However, we chose parameters that are typically seen from degenerate electron-gas and astrophysical systems such as pulsar magnetosphere and neutron stars $n_0 = 10^{23} - 10^{30} \text{ cm}^{-3}$ corresponding Fermi temperature $T_{Fe} = 10^4 - 10^9 \text{ K}$ and external magnetic field $B_0 = 10^4 - 10^{13} \text{ Gs}$ [6]. The separated spin evolution quantum hydrodynamic (SSE-QH) model is used in this study to investigate the linear and nonlinear characteristics of a magnetized spin quantum plasma consisting of electrons of both spin-up ($n_e \uparrow$) and spin-down ($n_e \downarrow$) concentrations and static ions forming a uniform neutralizing background. For simplicity, the exchange interaction is considered in the spin-down electrons population only. In the linear analysis, four modes have been observed; UHW (at the highest frequency), LW (starts at the plasma frequency), SSECW, and SSEAW (at the lowest frequency). It has been observed that the phase velocities of SSEAW

and SSECW decrease while that of LW and UHW increase with higher values of polarization ratio. Furthermore, the phase velocities of SSEAW and SSECW enhance while that of LW and UHW remain constant with increasing values of plasma number density. We used the reductive perturbation technique (RPT) to obtain the ZK-type equation. It is observed that our magnetized spin quantum plasma admits rarefactive soliton whose amplitude remains constant while whose width increases with the increasing strength of the applied magnetic field. It has also been observed that the amplitude of the soliton decreases while its width increases with increasing values of polarization ratio. The unstable region increases with the increase in polarization ratio and decreases with increasing magnetic-field strength and plasma number density. The instability growth rate γ decreases with the increasing values of κ and increases with the increase in the plasma number density and applied magnetic-field strength.

-
- [1] M. N. Rosenbluth, *Phys. Today* **13**, 27 (1960).
 [2] D. Pines, *J. Nucl. Energy, Part C* **2**, 5 (1961).
 [3] J. Zhu, X. Liu, and Y. Luo, *J. Plasma Phys.* **87**, 755870401 (2021).
 [4] G. Brodin, M. Marklund, and G. Manfredi, *Phys. Rev. Lett.* **100**, 175001 (2008).
 [5] P. K. Shukla and B. Eliasson, *Rev. Mod. Phys.* **83**, 885 (2011).
 [6] A. K. Harding and D. Lai, *Rep. Prog. Phys.* **69**, 2631 (2006).
 [7] M. Marklund and G. Brodin, *Phys. Rev. Lett.* **98**, 025001 (2007).
 [8] Z. Iqbal, U. Khanum, and G. Murtaza, *Contrib. Plasma Phys.* **59**, 284 (2019).
 [9] L. S. Kuzmenkov and S. G. Maksimov, *Theor. and Math. Phys.* **118**, 287 (1999).
 [10] M. V. Kuzlev and A. A. Rukhadze, *Phys. Usp.* **42**, 603 (1999).
 [11] L. S. Kuz'menkov, S. G. Maksimov, and V. V. Fedoseev, *Russ. Phys. J.* **43**, 718 (2000).
 [12] L. S. Kuzmenkov, S. G. Maksimov and V. V. Fedoseev, *Theor. Math. Phys.* **126**, 258 (2001).
 [13] L. S. Kuz'menkov, S. G. Maksimov, and V. V. Fedoseev, *Theor. Math. Phys.* **126**, 212 (2001).
 [14] G. Brodin and M. Marklund, *New J. Phys.* **9**, 277 (2007).
 [15] G. Brodin and M. Marklund, *Phys. Plasmas* **14**, 112107 (2007).
 [16] Z. Iqbal, M. Younas, I. A. Khan, and G. Murtaza, *Phys. Plasmas* **26**, 112101 (2019).
 [17] A. P. Misra, G. Brodin, M. Marklund, and P. K. Shukla, *New J. Phys.* **76**, 857 (2010).
 [18] M. Stefan, J. Zamanian, G. Brodin, A. P. Misra, and M. Marklund, *Phys. Rev. E* **83**, 036410 (2011).
 [19] P. A. Andreev, L. S. Kuzmenkov, and M. I. Trukhanova, *Phys. Rev. B* **84**, 245401 (2011).
 [20] P. A. Andreev, *Ann. Phys. (NY)* **350**, 198 (2014).
 [21] P. A. Andreev, *Phys. Rev. E* **91**, 033111 (2015).
 [22] P. A. Andreev and L. S. Kuzmenkov, *Appl. Phys. Lett.* **108**, 191605 (2016).
 [23] P. A. Andreev, *Phys. Plasmas* **23**, 012106 (2016).
 [24] R. Ahmad, N. Gul, M. Adnan, and F. Y. Khattak, *Phys. Plasmas* **23**, 112112 (2016).
 [25] Z. Iqbal and P. A. Andreev, *Phys. Plasmas* **23**, 062320 (2016).
 [26] N. Gul, Ikramullah, R. Ahmad, M. Adnan, and F. Y. Khattak, *Phys. Scr.* **95**, 045603 (2020).
 [27] J. Zamanian, M. Marklund and G. Brodin, *Phys. Rev. E* **88**, 063105 (2013).
 [28] M. Akbari-Moghanjoughi, *Phys. Plasmas* **21**, 032110 (2014).
 [29] P. A. Andreev and A. Y. Ivanov, *Phys. Plasmas* **22**, 072101 (2015).
 [30] M. I. Trukhanova and P. A. Andreev, *Phys. Plasmas* **22**, 022128 (2015).
 [31] N. Gul and R. Ahmad, *Phys. Scr.* **96**, 055602 (2021).
 [32] Z. Rahim, M. Adnan, and A. Qamar, *J. Phys. Soc. Jpn.* **89**, 094502 (2020).
 [33] P. Nozieres and D. Pines, *Phys. Rev.* **111**, 442 (1958).
 [34] H. Kanazawa, S. Misawa, and E. Fujita, *Prog. Theor. Phys.* **23**, 426 (1960).
 [35] S. Datta and R. L. Gunshor, *J. Appl. Phys.* **54**, 4453 (1983).
 [36] Y. D. Jung and M. A. Moghanjoughi, *Phys. Plasmas* **21**, 032108 (2014).
 [37] G. W. Lee and Y. D. Jung, *Phys. Plasmas* **20**, 062108 (2013).
 [38] M. A. Allen and G. Rowlands, *J. Plasma Phys.* **50**, 413 (1993).
 [39] M. A. Allen and G. Rowlands, *J. Plasma Phys.* **53**, 63 (1995).
 [40] F. Haas, G. Manfredi, and M. Feix, *Phys. Rev. E* **62**, 2763 (2000).
 [41] G. Manfredi and F. Haas, *Phys. Rev. B* **64**, 075316 (2001).
 [42] T. Koide, *Phys. Rev. C* **87**, 034902 (2013).
 [43] L. S. Kuz'menkov, S. G. Maksimov and V. V. Fedoseev, *Theor. Math. Phys.* **126**, 110 (2001).
 [44] G. Brodin, A. P. Misra, and M. Marklund, *Phys. Rev. Lett.* **105**, 105004 (2010).
 [45] A. P. Misra, G. Brodin, M. Marklund, and P. K. Shukla, *Phys. Rev. E* **82**, 056406 (2010).
 [46] A. P. Misra, G. Brodin, M. Marklund, and P. K. Shukla, *Phys. Plasmas* **17**, 122306 (2010).
 [47] G. Brodin, A. Holkundkar, and M. Marklund, *J. Plasma Phys.* **79**, 377 (2013).
 [48] P. Kumar and N. Ahmad, *Laser Part. Beams* **38**, 159 (2020).
 [49] K. P. Das and F. Verheest, *J. Plasma Phys.* **41**, 139 (1989).

- [50] S. Rand, *Phys. Fluids* **7**, 64 (1964).
- [51] P. K. Shukla and B. Eliasson, *Phys. Usp.* **53**, 51 (2010).
- [52] J. Zamanian, M. Marklund and G Brodin, *New J. Phys.* **12**, 043019 (2010).
- [53] G. Brodin, M. Marklund, J. Zamanian, and M. Stefan, *Plasma Phys. Control. Fusion* **53**, 074013 (2011).
- [54] G. Brodin and J. Zamanian, *Rev. Mod. Plasma Phys.* **6**, 4 (2022).
- [55] G. Brodin, M. Marklund, J. Zamanian, A. Ericsson, and P. L. Mana, *Phys. Rev. Lett.* **101**, 245002 (2008).
- [56] H. Washimi and T. Taniuti, *Phys. Rev. Lett.* **17**, 996 (1966).
- [57] A. A. Mamun, *Phys. Scr.* **58**, 505 (1998).
- [58] A. A. Mamun, *J. Plasma Phys.* **59**, 575 (1998).
- [59] N. R. Kundu, M. M. Masud, K. S. Ashrafi, and A. A. Mamun, *Astrophys. Space Sci.* **343**, 279 (2013).
- [60] E. Infeld, *J. Plasma Phys.* **8**, 105 (1972).
- [61] E. Infeld and G. Rowlands, *J. Plasma Phys.* **10**, 293 (1973).